Myosin and Paramyosin Are Organized about a Newly Identified Core Structure

HENRY F. EPSTEIN, DAVID M. MILLER III, IRVING ORTIZ, and GARY C. BERLINER
Department of Neurology, Baylor College of Medicine, Houston, Texas 77030. Dr. Miller's present address is Department of Zoology, North Carolina State University, Raleigh, North Carolina 27606.

ABSTRACT Myosin isoforms A and B are differentially localized to the central and polar regions, respectively, of thick filaments in body wall muscle cells of *Caenorhabditis elegans* (Miller, D. M. III, I. Ortiz, G. C. Berliner, and H. F. Epstein, 1983, *Cell*, 34:477–490). Biochemical and electron microscope studies of KCl-dissociated filaments show that the myosin isoforms occupy a surface domain, paramyosin constitutes an intermediate domain, and a newly identified core structure exists. The diameters of the thick filaments vary significantly from 33.4 nm centrally to 14.0 nm near the ends. The latter value is comparable to the 15.2 nm diameter of the core structures. The internal density of the filament core appears solid medially and hollow at the poles. The differentiation of thick filament structure into supramolecular domains possessing specific substructures of characteristic stabilities suggests a sequential mode for thick filament assembly. In this model, the two myosin isoforms have distinct roles in assembly. The behavior of the myosins, including nucleation of assembly and determination of filament length, depend upon paramyosin and the core structure as well as their intrinsic molecular properties.

The body wall muscle cells of the nematode *Caenorhabditis elegans* contain two chemically and genetically distinct isoforms of myosin heavy chain, A and B. Immunocytochemical localization with both affinity purified and specific monoclonal antibodies shows that the two isoforms coexist in the same muscle cells and sarcomeres (13, 17). All isolated thick filaments react with the monoclonal antibodies of either specificity, indicating that the isoforms are contained within the same filaments. However, the A form is localized to the central 1.8 μm of the 9.7-μm-long filaments, whereas the B form is located in the polar region, but is absent in the central 0.9 μm of the filament (17). Fig. 1 is a schematic diagram showing locations of the A and B heavy chains and examples of thick filaments that were reacted with the specific antibodies. The surface of nematode thick filaments is differentiated by myosin isoform content into five zones.

The locations of the myosin heavy chain isoforms in this model explain several independent observations regarding nematode body wall myosins. Previous studies of nematode myosins indicate that native molecules are homodimers of either heavy chain isoform; no heterodimers are detected (21, 22). The different locations of the heavy chain types imply that the myosin molecules within thick filaments are primarily homodimers. The ratio of B to A heavy chains appears constant, whereas their amounts increase 40-fold during the post-embryonic stages of the nematode life cycle (4). This fixed ratio, ~4:1 (28), is consistent with the distributions of the two forms in the thick filaments shown in Fig. 1.

The different locations of myosins A and B have important structural correlations. The central regions that contain only myosin A are the regions in which myosin molecules pack in a bipolar fashion to form the bare zone. This zone probably contains the site for initiation of myosin assembly. In this same region, M-line structures cross-link thick filaments to produce the ordered lattice of the A band. According to the model of Miller et al. (17), only myosin A would be involved in these interactions. In contrast, myosin B molecules of the flanking regions pack only in a polar manner. This suggests that the elongation and termination reactions of assembly involve only myosin B.

The experiments described in this paper provide additional evidence confirming our previous observations and model. They also explore the structural basis of this molecular differentiation of the body wall thick filaments. The major approach of the experiments is the processive dissociation of isolated thick filaments by increasing KCl concentration and the concomitant solubilization of myosin and paramyosin. Electron microscopy of dissociated filaments and their com-

THE JOURNAL OF CELL BIOLOGY · VOLUME 100 MARCH 1985 904-915

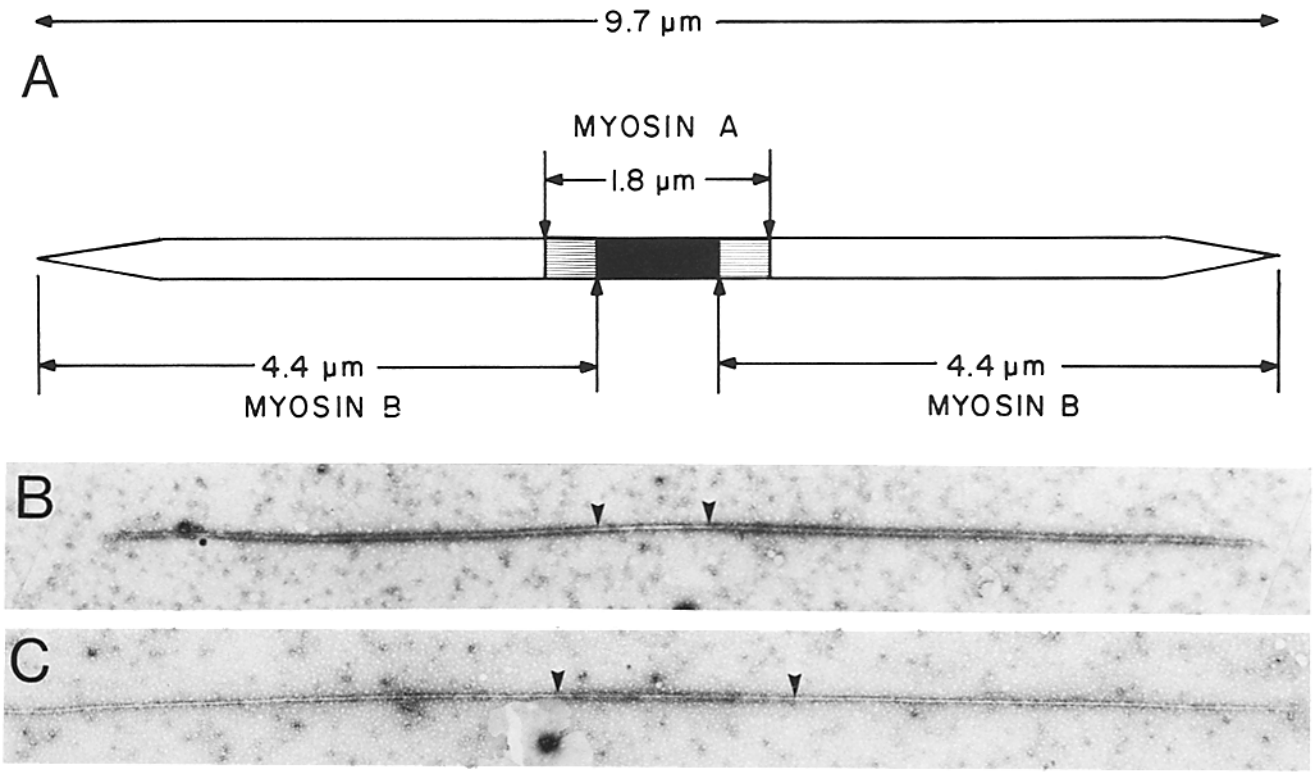

FIGURE 1 Proposed locations of myosins A and B in thick filaments of body wall muscle cells. (*A*) Schematic diagram, accurate for length of the locations (1). The electron micrographs (*B* and C) are of localizations with the antimyosin B, 28.2, and antimyosin A, 5.6, monoclonal antibodies, respectively. The arrows in *B* flank the gap of 28.2 labeling. The arrows in C include the zone of 5.6 reaction. The diagrams are adapted from Miller et al. (17), with permission of MIT Press.

plexes with specific antibodies confirms the previous localizations of myosins A and B in native filaments. A central stub containing myosin A remained at 0.45 M KCl. The polar regions that contained myosin B disappeared. Underlying the organization of the myosin-containing surface domain into its subdomains were two other supramolecular domains: one of intermediate volume that contained paramyosin and a newly identified core structure. The thick filaments tapered continuously from the central region to the ends of the polar regions. The tapering suggests that the myosin and paramyosin domains were changing structurally. The internal densities of the cores decreased in correlation with the tapering. The relative stabilities of the three domains and the changes in substructure with length suggest a specific pathway for the assembly of thick filaments.

MATERIALS AND METHODS

Nematode Growth and Strains: Wild-type N2 strains of *Caenorhabditis elegans* were grown on peptone-enriched nematode growth medium (21).

Antibodies: The monoclonal antibodies used in these studies are as previously reported (3, 17).

Electron Microscopy of Thick Filaments: Thick filaments were prepared and examined as described previously (17) with two modifications. Frozen nematode suspensions were sectioned to 16-μm-thick slices. Formvar-coated carbon grids were glow discharged immediately before use. Length and diameter dimensions were measured from calibrated negatives with a dissecting microscope (Wild Heerbrügg Instruments, Inc., Farmingdale, NY) at 250× and an eyepiece micrometer.

KCl Dissociation of Thick Filaments: Isolated filaments were incubated overnight at 0°C in fresh relaxing buffer (10 mM $MgCl_2$, 1 mM EDTA, 5 mM ATP, 100 mM KCl, and 6.7 mM potassium phosphate [pH 6.35]). They were resuspended gently with a Pasteur pipette, and the solutions were permitted to settle for 5 min. The supernatant was divided into five equal volumes. Each volume was mixed with an equal volume of relaxing buffer modified so that $MgCl_2$ was 1 mM, and different final KCl concentrations were reached (0.1, 0.25, 0.35, 0.45, and 0.75 M KCl, respectively). The resuspension and mixing were performed as slowly and gently as possible in order to reduce shearing of the thick filaments to a minimum. The filament-KCl solutions were incubated at 0°C for 30 min.

Myosin and Paramyosin Content of Dissociated Thick Filaments: Equal volumes of filaments treated with different concentrations of KCl were centrifuged at 100,000 *g* for 30 min in a swinging bucket rotor (model SW 50.1; Beckman Instruments, Inc., Fullerton, CA). The supernatants were removed carefully without disturbing the pellets. Both supernatants and pellets were prepared for sodium dodecyl sulfate-polyacrylamide gel electrophoresis (2), and special care was taken to maintain all pellet and supernatant volumes equal within each class. All heating was performed in sealed Eppendorf tubes to avoid loss of solutions. 15-μl aliquots of either matched pellet or matched supernatant sets were electrophoresed simultaneously on 7.5% polyacrylamide-sodium dodecyl sulfate slab gels. To standardize gels for quantitation, a set of serially diluted purified nematode myosin samples was also electrophoresed on each gel. The myosin heavy chains of the purified myosin samples were used as internal standards for determining the myosin heavy chain and paramyosin contents of the experimental filament supernatants and pellets. The slab gels were run at 20 mA for stacking and 40 mA for separation until the bromphenol blue dye was 1 cm from the bottom of the 14-cm-long slab. The slab gels were stained in 0.1% (wt/vol) Coomassie brilliant blue and destained in 50% (vol/vol) methanol/5% (vol/vol) acetic acid until the backgrounds were clear. Wet gel slabs were scanned on a densitometer (Kontes Co., Vineland, NJ). The recordings were reproduced, cut out, and weighed.

RESULTS

Processive Solubilization of Myosin and Paramyosin from Thick Filaments

Thick filaments isolated from mammalian skeletal muscles can be solubilized processively from the distal tips toward the central bare zone by treatment with solutions of increasing KCl concentration (19, 25). In the case of skeletal muscles,

myosin is the major protein solubilized during this procedure. Nematode thick filaments like those of other invertebrate muscles contain paramyosin as a major protein component in addition to myosin (Fig. 2*A*). Paramyosin is believed to be internal to myosin in the filament backbone (24).

We initiated salt-dissociation experiments with nematode thick filaments in order to study the relationships between their substructure and their major proteins, the myosin isoforms and paramyosin. Fig. 2 shows that both the myosin heavy chain- and the paramyosin monomer-contents of sedimentable structures decreased as the KCl concentration increased. In a complementary fashion, the amounts of soluble myosin and paramyosin increased (Fig. 2*B*). Interestingly, the paramyosin was protected from proteolytic cleavage when in an assembled form within the filament, but became relatively susceptible to cleavage when soluble (6, 11). Actin and tropomyosin in the form of thin filaments were present as contaminants. Additional polypeptides were observed as minor bands. It has not been determined whether these proteins were contaminants, like the thin filament proteins, or represented significant components of thick filaments.

Densitometry of the myosin heavy chain and paramyosin permitted quantitative analysis of the solubilization. Fig. 3 shows that dissociation and solubilization of the two proteins underwent sharp transitions between 0.1 and 0.45 M KCl. At a KCl concentration of ~0.3 M, 50% soluble and 50% sedimentable molecules were obtained for both proteins. At 0.75

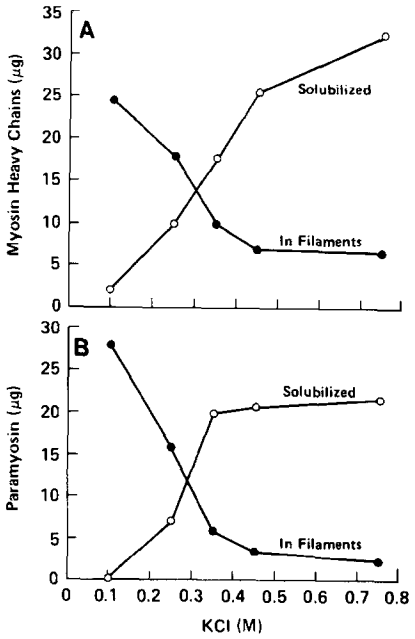

FIGURE 3 Behavior of myosin heavy chains and paramyosin during thick filament dissociation. Filled and hollow circles represent sedimentable and soluble myosin heavy chain (*A*) and paramyosin (*B*). The data of these graphs were derived from densitometry of gels as in Fig. 2.

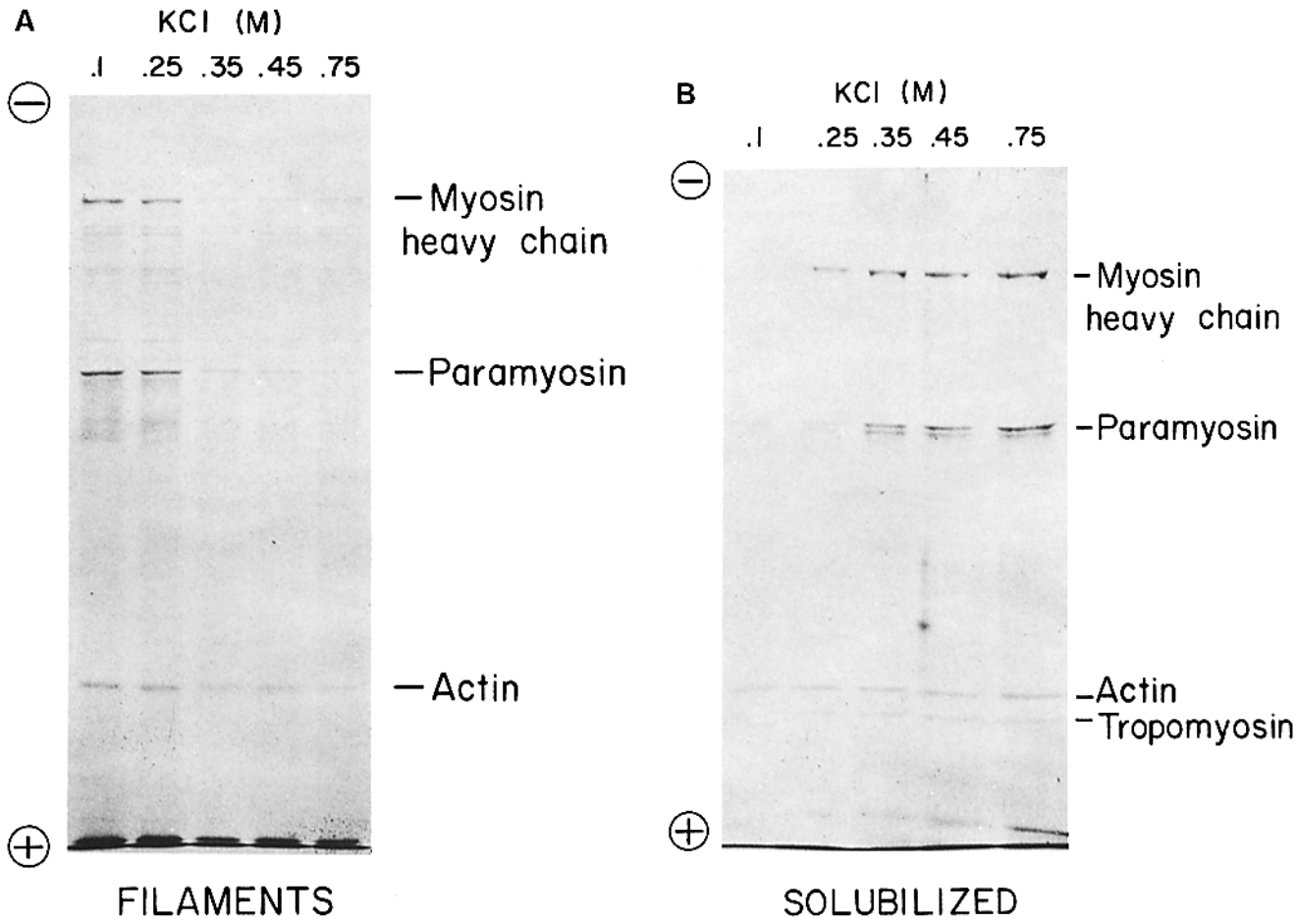

FIGURE 2 Gel electrophoresis of dissociated thick filaments. 7.5% polyacrylamide-SDS gels labs of sedimentable (*A*) and soluble (*B*) protein were run. The samples were obtained from centrifugation of filaments at the indicated KCl concentrations.

M KCl, pH 6.35, 80% of the myosin and 95% of the paramyosin were solubilized. The remaining structures retained ~20% of the myosin, and at most, 5% of the paramyosin originally in the thick filaments. Similar results were obtained in multiple experiments.

Structures of filaments after treatment at various KCl concentrations were examined by electron microscopy. The regions containing myosins A and B were identified by reactions with the specific monoclonal antibodies 5.6 and 28.2, respectively (17) (see below). The lengths of overall filaments and of the antibody-labeled zones were measured for many filaments at each concentration of KCl. Fig. 4 shows the measured lengths as functions of KCl concentration. At 0.1 M KCl, the mean filament length and the length of myosin-containing structures were identical. The two functions began to diverge at 0.25 M KCl. The measured lengths of myosin-containing zones followed a function that is qualitatively similar to the dissociation curves for both myosin heavy chain and paramyosin in Fig. 3. The final mean lengths of antibody-labeled structures, ~0.9 μm, were similar to the central all-myosin A zone mean length of Fig. 1. The fraction of myosin heavy chain that remained at 0.75 M KCl, 0.2, was similar to the fraction of body wall myosin that is myosin heavy chain A (28).

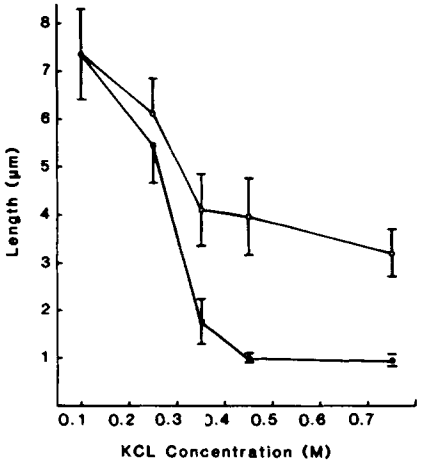

FIGURE 4 Lengths of filaments and myosin-containing zones during KCl dissociation. The means and standard deviations of these lengths are plotted as functions of KCl concentrations. Filled circles represent lengths of myosin-containing zones, and hollow circles represent the lengths of the entire filaments including the myosin-containing zones.

In contrast, the overall lengths of the filaments were significantly longer than the myosin-containing regions at 0.35 M KCl and higher concentrations. The final mean overall length, ~3.2 μm, suggests that substantial structures of some kind were present under conditions in which very little paramyosin remained, and myosin appeared restricted to smaller portions of the filaments.

Ultrastructural Examination of Dissociated Thick Filaments

Under dissociating conditions in which myosin B and paramyosin were solubilized or were restricted to particular segments, the more extended lengths of the overall filaments suggest that core structures distinct from the myosin- and paramyosin-containing domains of nematode thick filaments were present. The cores appeared at the polar ends of filaments and through most, if not all, of the lengths of the filaments. These core structures had a mean diameter of 15.2 ± 1.8 nm (n = 219).

Electron microscopy shows long filaments at 0.25 M KCl (Fig. 5, *A* and *B*). Such structures are typical of thick filaments under these conditions. The regions near the ends of these filaments appeared smoother and narrower than the rest of the structures. Examination at higher magnification confirmed these observations. Fig. 5, *C* and *D*, shows that the

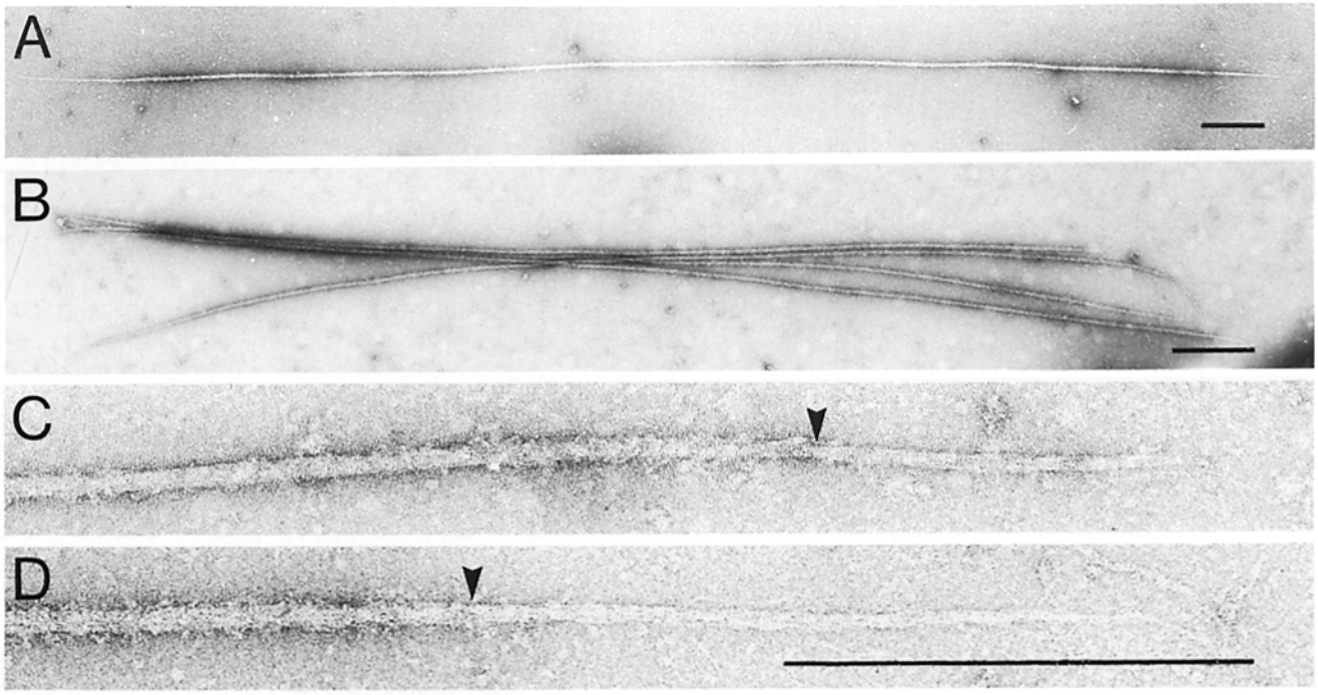

FIGURE 5 Electron microscopy of thick filaments of 0.25 M KCl. The smooth appearance of the exposed cores at the ends differ from the rough-appearing myosin projections along the rest of the filaments. The transitions are marked by arrows. Bars, 0.5 μm.

ends were distinctly smoother and smaller in diameter than the central regions. The rough appearance is characteristic of the myosin surfaces of thick filaments from nematodes and other sources (11, 12).

Rare filaments at 0.25 M KCl, pH 6.35, represented a different kind of structural intermediate with paramyosin at its surface. Fig. 6 *A* depicts a filament that appeared subdivided into three zones. In the middle (between the arrows), the filament had a rough appearance, typical of a myosin surface. At the large arrow, a transition was observed. This rightmost region of the filament appeared paracrystalline and flattened. At the small arrow, another transition occurred. The leftmost region of the filament appeared smoother and narrower than the rest of the filament. Fig. 6, *B–D*, at higher magnification, showed transitions of the first kind. At the left of each of these filaments were typical myosin surfaces. At the right, following transition regions of slightly smaller diameters than intact filaments, were paracrystalline structures that flattened as they extended from the transition points. These polymorphic structures closely resembled many of the paracrystals of nematode paramyosin (Fig. 6, *C* and *D*) (6, 26) and the nodal appearance of the paramyosin domains of dissociated molluscan thick filaments (Fig. 6 *B* and 12 *D*) (24). These paracrystalline structures were not detected at higher salt concentrations that solubilized most of the paramyosin. The contiguity of myosin-containing regions of native diameter with these paramyosin structures makes unlikely the possibility that these paracrystals formed in vitro from solubilized paramyosin. Such contiguous structures were not observed when purified myosin and paramyosin were co-precipitated in vitro (6). We concluded that these structures represented an intermediate paramyosin-containing domain. The distinct appearance of the more narrow structures from either the myosin surfaces or the paramyosin paracrystalline structures again suggested that they represent a previously unidentified core structure.

This tentative conclusion was corroborated further by electron microscopy of nematode thick filaments after dissociation at higher KCl concentrations. Filaments were dissociated at 0.35 M KCl (Fig. 7, *A* and *B*), and at 0.45 M KCl (Fig. 7, *C* and *D*). In all four images, the myosin-containing central zones were distinguished clearly from the flanking, more narrow core structures. Higher magnification electron micrographs of filaments at 0.35 M KCl (Fig. 7 *E*) and at 0.45 M KCl (Fig. 7 *F*) provided further details. The 0.35 M KCl-treated filaments have myosin zones measuring ~1.8 μm long, whereas the 0.45 M KCl-treated filaments have more restricted myosin zones, ~0.9 μm. Lengths based upon negative-staining characteristics of myosin agree with the antibody labeling of similarly treated filaments (Fig. 4). The shortened mean overall length of dissociated filaments was probably the result of the fragility of the exposed core structures. The dissociated filaments of Fig. 7, *A–D* were chosen because their lengths approached the length of native, intact filaments.

Close examination of core structures such as in Fig. 7 *F* revealed some penetration of stain in their centers. These observations were consistent with the hypothesis that core structures could be partially filled tubes. Electron micrographs of cross-sections supported this hypothesis and are described below.

Reactions of Specific Monoclonal Antibodies with Dissociated Thick Filaments

Dissociated thick filaments were reacted with specific monoclonal antibodies to confirm the proposed location of the two myosins under conditions in which the structural constraints of native filaments might be relaxed and to test for the presence of known major protein components as antigens in the core structures.

Fig. 8 shows the reaction of the antimyosin B-specific

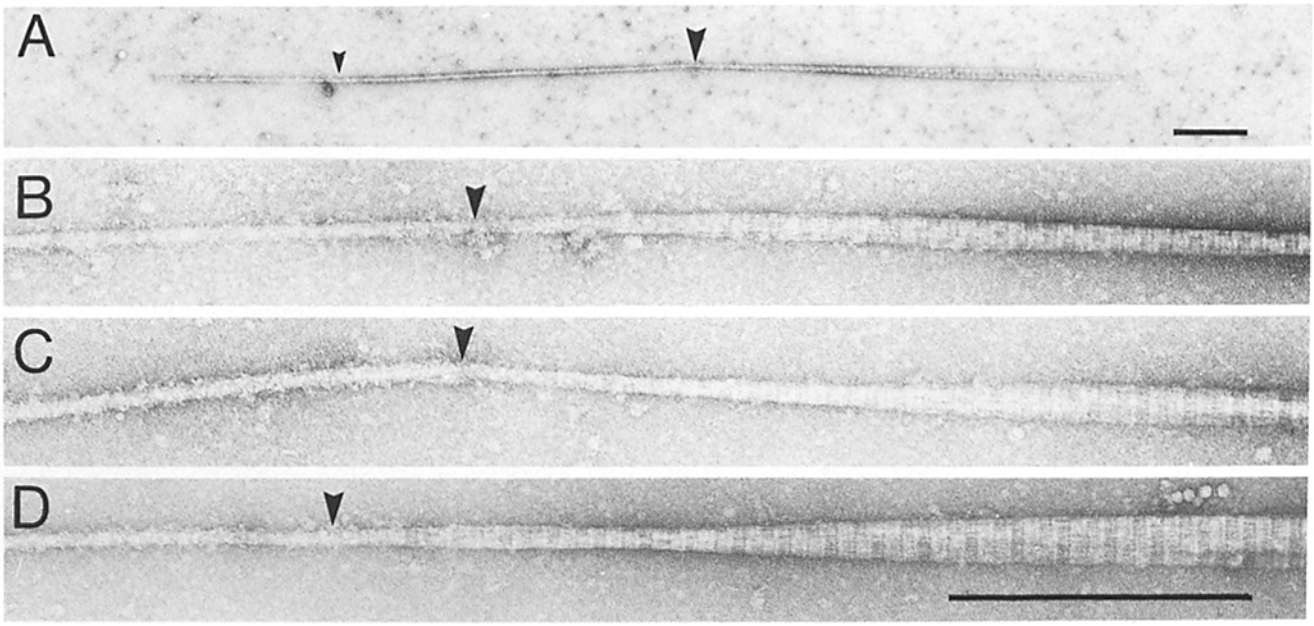

FIGURE 6 Paracrystalline regions of thick filaments at 0.25 M KCl. These regions resemble different paracrystalline forms of nematode paramyosin. In each micrograph, the paracrystalline regions on the right differ markedly from the rough-appearing, myosin-containing regions on the left. These transitions are marked by arrows. In the uppermost micrograph (*A*), an exposed smooth core structure, a myosin zone, and an exposed paramyosin region are observed from left to right. The small arrow marks the first transition, and a large arrow marks the latter transition. Bars, 0.5 μm.

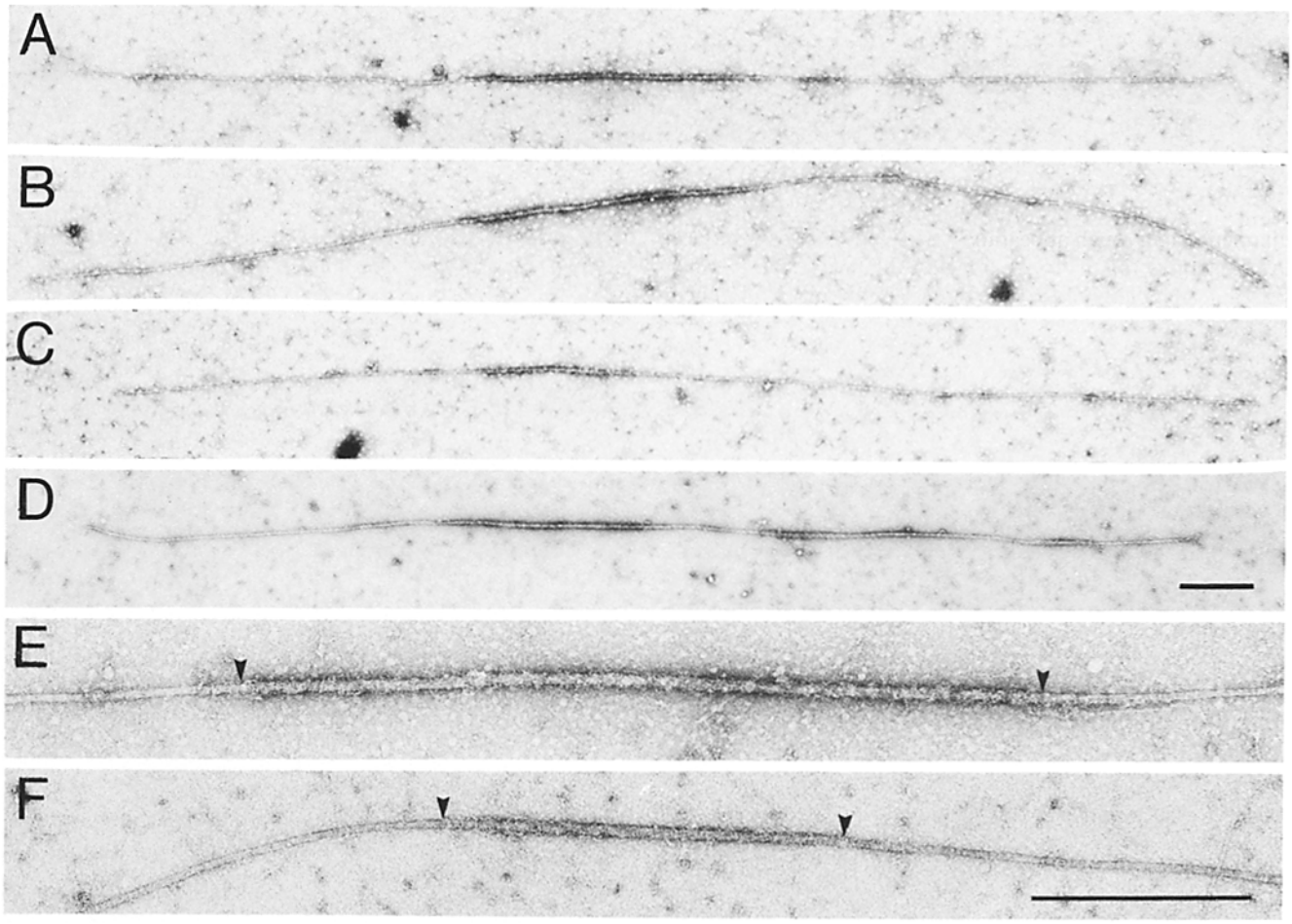

FIGURE 7 Electron microscopy of thick filaments dissociated at 0.35 and 0.45 M KCl. Micrographs are of filaments dissociated at 0.35 M (*A*, *B*, and *E*) and 0.45 M (*C*, *D*, and *F*) KCl. In *E* and *F*, the myosin-containing regions are between each pair of arrows. Note the long expanses of exposed cores in the lower magnification micrographs. The 0.45-M KCl-treated filaments have smaller myosin regions than the 0.35-M KCl-treated filaments. Bars, 0.5 μm.

monoclonal antibody, 28.2, with thick filaments at three stages of dissociation. Fig. 8, *A* and *B* depicts the ends of thick filaments in 0.25 M KCl. The exaggerated rough appearance of the myosin-containing regions on the left were typical of antibody labeling. The exposed core structures to the right did not react with the antimyosin B antibody.

Fig. 8, *C* and *D*, confirmed that myosin B was localized in the flanking regions of the central myosin-containing regions at 0.35 M KCl but not in the most central 0.9 μm. These localizations were in agreement with the experiments of Miller et al. (17) with native filaments. At 0.45 M KCl, the myosin-containing zones were limited to the central 0.9 μm and did not react with antimyosin B (Fig. 8, *E* and *F*). At both 0.35 and 0.45 M KCl, the core structures did not react with the 28.2 antibody, indicating that myosin B was not present antigenically in the core structures.

Fig. 9 shows the reaction of the antimyosin A-specific monoclonal antibody, 5.6, with isolated nematode thick filaments at 0.25, 0.35, and 0.45 M KCl. An antibody-labeled thick filament treated with 0.25 M KCl is shown in Fig. 9*A*. The labeling of the central 1.8 μm was identical to the reaction of 5.6 antibody with native filaments. Thick filaments that had been dissociated at 0.35 M KCl and reacted with antimyosin A (Fig. 9, *B* and *C*) showed labeled regions of similar length, ~1.8 μm, to the myosin-containing regions at 0.35 M KCl (Fig. 7, *A* and *B*) and to the labeled regions at 0.25 M KCl (Fig. 9*A*). Fig. 9, *D* and *E*, showed similarly labeled filaments dissociated at 0.45 M KCl. The lengths of the reacted zones, ~0.9 μm, were similar to the myosin-containing regions of Fig. 7*F* under similar conditions and were interpreted to be all myosin A zones. These reactions may be compared with the absence of reaction between the 28.2 antibody and 0.45 M KCl filaments of Fig. 8, *E* and *F*.

The micrographs of filaments treated with 0.35 and 0.45 M KCl in Fig. 9, *B–E* showed that the antimyosin A antibody did not react with the core structures emanating from the central regions. Therefore, myosin A was not present antigenically in the core structures. The core structures of nematode thick filaments after dissociation at 0.35 and 0.45 M KCl have been incubated with monoclonal antibodies 5.9 and 5.23 that are specific to paramyosin (3). No labeling of the core structures occurred whereas the same antibodies labeled paramyosin paracrystals. Thus, paramyosin was not present antigenically in the core structures.

Ultrastructural Examination of Thick Filaments in Nematode Body Wall Muscle Cross-sections

Fig. 10 is a cross-sectional micrograph of a nematode body wall muscle sarcomere from the central third of the organism.

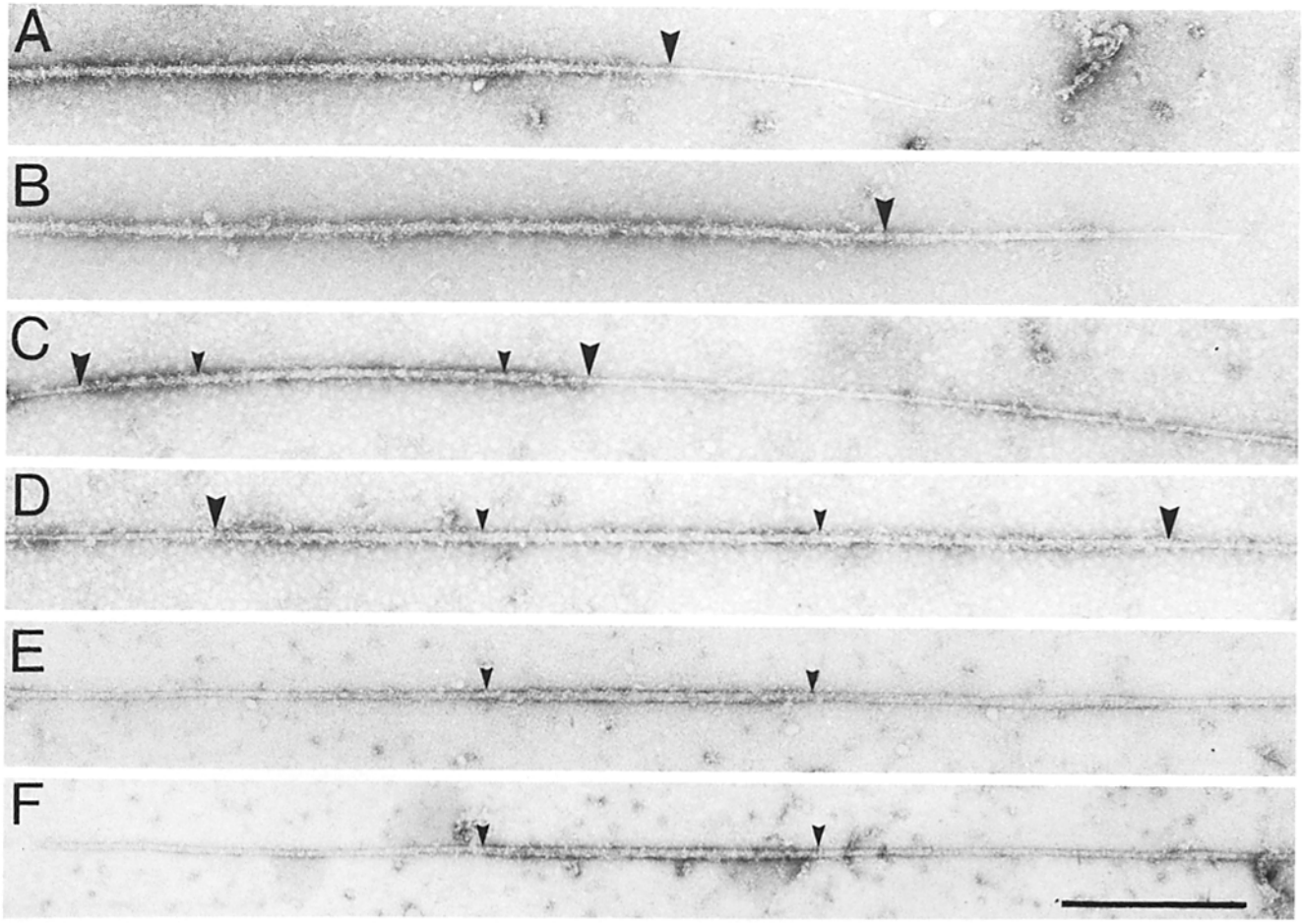

FIGURE 8 Reactions of antimyosin B antibodies with dissociated filaments. Antimyosin B monoclonal antibodies, 28.2, were reacted with thick filaments treated previously with 0.25 M KCl (*A* and *B*); the zones of reaction are to the left of each arrow, 0.35 M KCl (*C* and *D*); the reaction zones are between each pair of arrows; and 0.45 M KCl (*E* and *F*), the myosin-containing zone (no reaction), is between the arrows. Note the absence of antibody labeling at 0.45 M KCl. Bars, 0.5 μm.

In the obliquely striated muscles of nematode body wall, a cross-section samples thick filaments at different positions along their length: At the A-I band interfaces, the polar ends of thick filaments are cross-sectioned; at the center of the A band in the H zone where no thin filaments are present, the central regions of thick filaments are cross-sectioned; and, at intermediate portions of the A bands, regions of the thick filament between the central and polar end regions are sampled (30). When cross-sectional profiles of thick filaments were sampled in this way, two striking features were apparent. The diameters of filaments near their centers were significantly larger than near their ends. This marked tapering has been noted previously (26), but its structural significance was not discussed. The filaments appeared solid in the central regions and hollow near the polar ends with intermediate densities along the way. Such a change in internal structure has been noted in thick filaments in nematode pharyngeal muscles. Several previously published micrographs of the body wall muscles (2, 14, 15, 27) show similar images at lower magnification. Double staining with phosphotungstate in addition to uranyl acetate also produced a difference in core density but of smaller magnitude. Millman and Bennett (18) also find a similar effect with scallop striated adductor muscle thick filaments.

Fig. 11 demonstrates the quantitative aspects of thick filament tapering as a function of calculated distance from the center according to the model of Mackenzie and Epstein (11). Each point is the mean of 20–40 measurements from the same region as the micrograph of Fig. 10. The values in Fig. 11 represent measurements based upon distance from the H zone. The standard deviations (±10–20% of the individual means) indicate that there is significant variability about these means. Modeling of these values was dependent upon the assumption of a well-ordered lattice. The thick filament array of nematode body wall muscles shows only short-range ordering. Therefore, some mixing of lattice planes was likely to have occurred in the sampling of Fig. 11, and the total decrease in diameters was probably greater. Therefore, 10 filaments were selected from the most central regions near a clear M line. The mean diameter of these cross-sectioned filaments was 33.4 nm. The mean diameter of 10 filaments selected from the most polar regions was ~14 nm.

The diameter of filaments sectioned near their ends was slightly less than the diameter of the negatively stained isolated core structures, ~15.2 nm. These results suggest that the myosin and paramyosin domains were tapering specifically, whereas the cores remained constant in diameter over most of the filament length. The hollow or partially hollow nature of the filament cores as suggested by the cross-sections is consistent with the penetration of isolated core structures by negative stain observed in some dissociated thick filaments. The widest portions of the thick filaments with solid cores

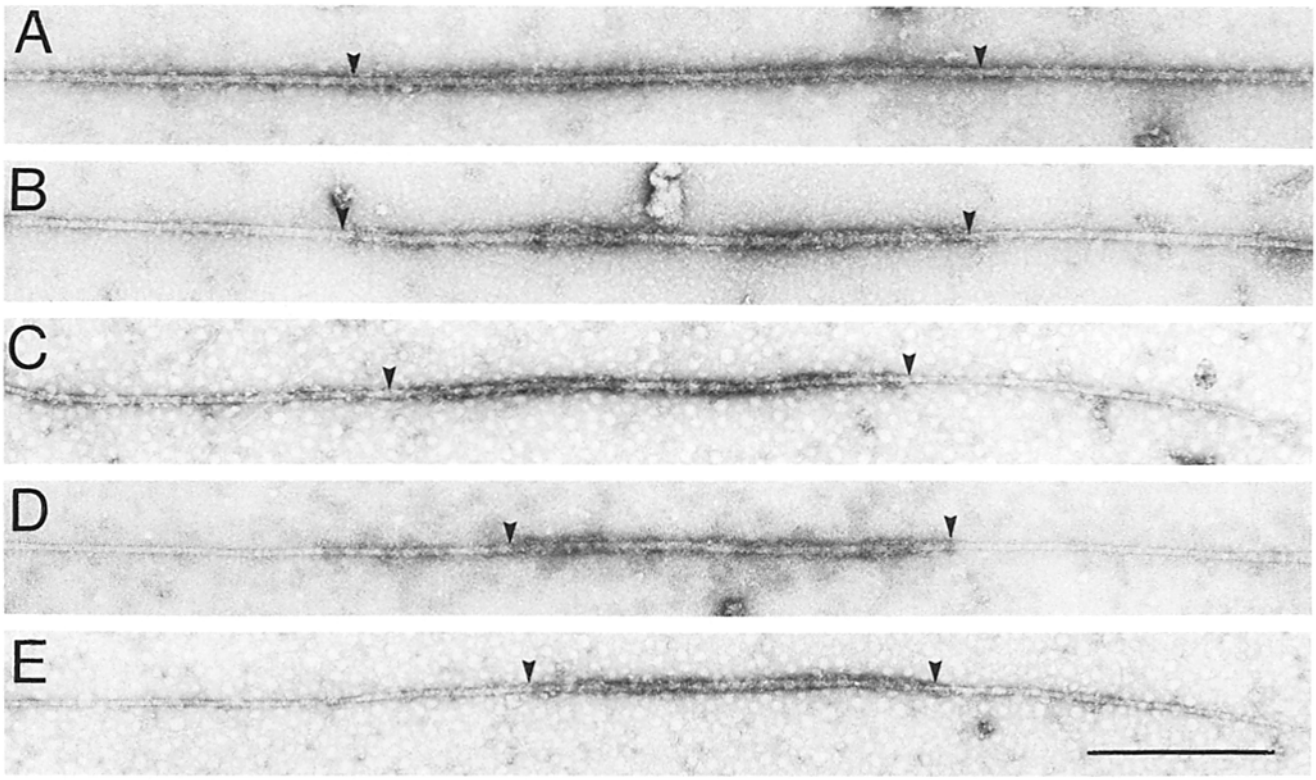

FIGURE 9 Reactions of antimyosin A antibodies with dissociated thick filaments. Antimyosin A monoclonal antibodies, 5.6, were reacted with thick filaments treated previously with 0.25 M (*A*), 0.35 M (*B* and *C*) and 0.45 M (*D* and *E*) KCl. The reaction zones are between the arrows. Note the presence of reaction in all cases and the narrowing of the reaction zones at 0.45 M KCl. Bars, 0.5 μm.

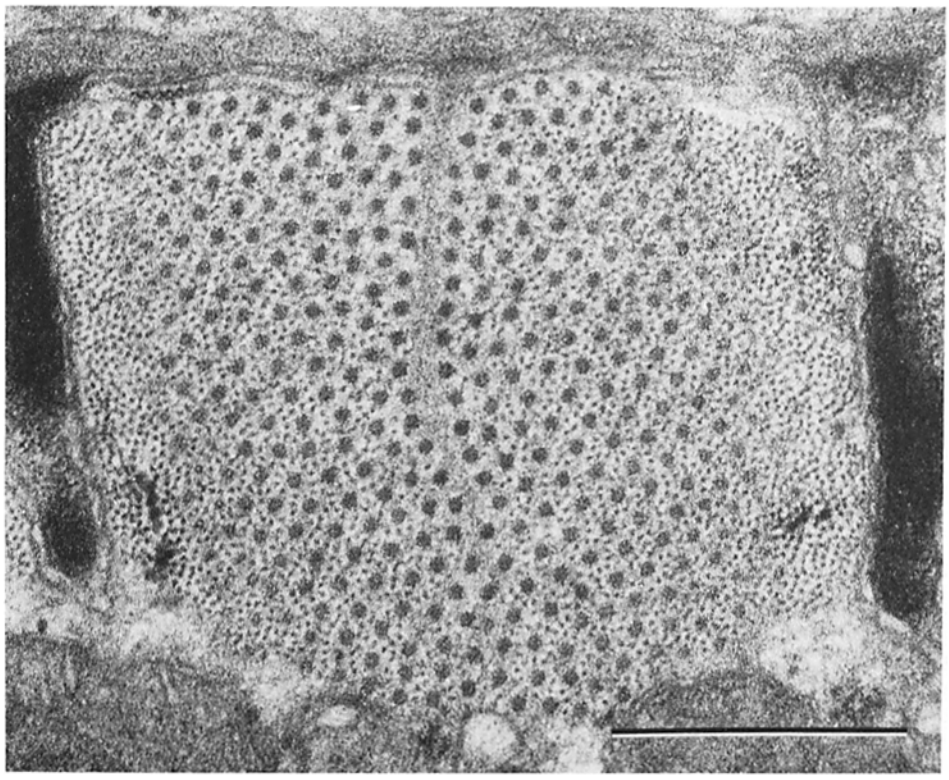

FIGURE 10 Cross-section of nematode body wall muscle. A sarcomere of the obliquely striated muscle exhibits I bands that contain thin filaments surrounding the A band that contains both thick and thin filaments. In the center of the A band, the H zone contains only thick filaments and a M line density. Compare the diameters and core densities of the thick filaments from the center to the periphery of the A band. Bar, 0.5 μm.

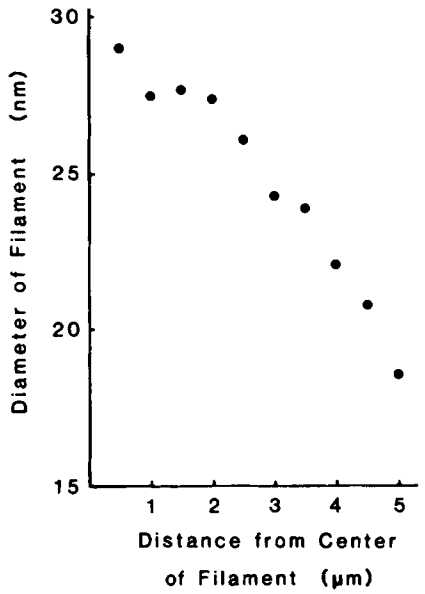

FIGURE 11 Quantitation of thick filament tapering. Micrographs similar to Fig. 10 were analyzed. The diameters of thick filaments were measured. The mean diameters of filaments at each distance were plotted as a function of calculated length from the center of the thick filaments. These calculations were derived from the measured distances from the centers of A bands according to the model of Mackenzie and Epstein (11).

were coincident with the regions containing myosin A, whereas the tapering portions of the thick filaments with cores of varying electron density were coextensive with the myosin B-containing regions. Over the last 0.1–0.3 μm of the thick filaments, the cores, too, must either taper or disappear because we have observed the ends of intact thick filaments with diameters of smaller than 15 nm to virtually zero in both negatively stained isolated filaments and positively stained sectioned filaments.

DISCUSSION

The thick filaments of body wall muscle cells of *Caenorhabditis elegans* can be dissociated processively by increasing concentrations of KCl. The known major protein components of the thick filaments, myosin and paramyosin, are solubilized to ~80 and 95%, respectively, by the KCl dissociation. Under the same conditions, smooth-looking structures of 15 nm diameter are revealed. These structures differ in morphological characteristics from the rough myosin or paracrystalline paramyosin surfaces (for a comparison, see Fig. 12) and do not react with monoclonal antibodies specific to either nematode body wall myosin or paramyosin. By their placement and diameter, these structures are termed polar core structures. They appear to be present along the lengths of the thick filaments from the polar ends to the central 0.9-μm zones and possibly along the entire lengths. In the polar regions, paramyosin forms a domain intermediate between the core structure and the myosin surface (Fig. 13). These three domains would be coaxial.

The localizations of myosins A and B by reactions of isoform-specific monoclonal antibodies with restricted portions of dissociated thick filaments described in this paper agree with the results of similar antibody reactions with native filaments (17). The specific antimyosin A antibody, 5.6, reacts only with the central 1.8-μm region of dissociated filaments

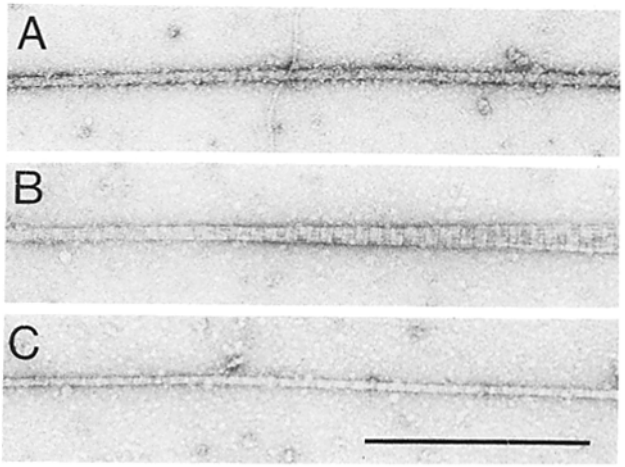

FIGURE 12 Electron microscopy of myosin, paramyosin, and core structures. Native filament at 0.1 M KCl (*A*) shows myosin surface. Filament dissociated at 0.25 M KCl (*B*) shows paramyosin domain. Filament dissociated at 0.35 M KCl (C) shows core structure. Bar, 0.5 μm.

and not with more polar zones. The specific antimyosin B antibody, 28.2, reacts with the more polar regions of dissociated filaments but not with the most central 0.9-μm zone. At 0.45 M KCl, the only myosin-containing region that remains is the 0.9-μm zone. Only antimyosin A labels these regions of 0.45 M-treated filaments; antimyosin B does not react with them. Therefore, the surface myosin domain is differentiated into subdomains that differ by their myosin isoform content as indicated in Fig. 13.

The structure of these supramolecular domains is not constant. The tapering of the thick filaments that results in decreased overall diameters from 33.4 to 14.0 nm (as determined by positive staining) has important implications for the nature of molecular packing in these domains. The core structures appear to have relatively constant diameters of 15 nm except at the very ends when examined as portions of negatively stained dissociated filaments. The similarity in diameter of the most polar regions of thick filaments in positively stained, cross-sectioned, embedded, and fixed material (14.0 nm), and of the negatively stained isolated polar core structures (15.2 nm), suggests that the myosin and paramyosin domains must be depleted or actually not remain as continuous domains near the ends of the filaments. This conclusion agrees with electron microscopy of negatively stained isolated thick filaments, in which the most polar (0.1–0.3 μm) appear smooth. Therefore, both the packing of myosin and paramyosin molecules and the number of these protein molecules per unit length must be changing significantly as the thick filaments taper. Since the tapering appears continuous over the long polar regions (4.4 μm/side), unitary models of the kinds discussed by McLachlan and Karn (16), Squire (23), or Wray (29), although useful, cannot be strictly correct for all regions of the filaments.

The amount of the myosin and paramyosin released and the lengths of remaining myosin- and paramyosin-containing regions agree with modeling of the myosin and paramyosin contents expected from the measured tapering (Honda, S., unpublished observations). Such a model is depicted in a highly schematic form in Fig. 14. The model assumes that at the ends of the central 1.8-μm subdomain the overall diameter is 31 nm. At these junctions, the myosin and paramyosin

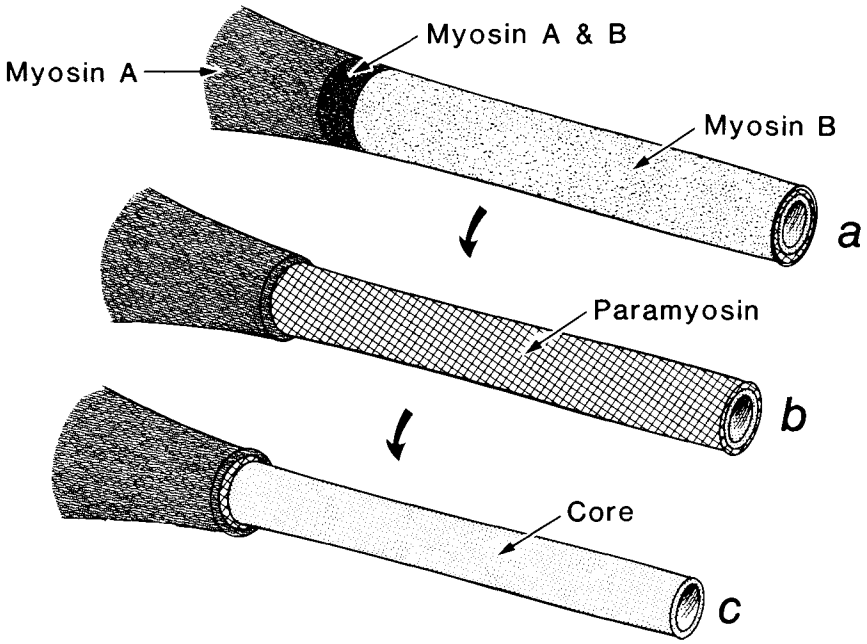

FIGURE 13 Model of thick filament domains. *a* depicts a portion of an intact native filament. In *b*, the myosin B subdomain has been removed. In *c*, myosin B and paramyosin have been removed. The myosin B and paramyosin domains are coaxial with the core structure in the polar regions of the thick filament.

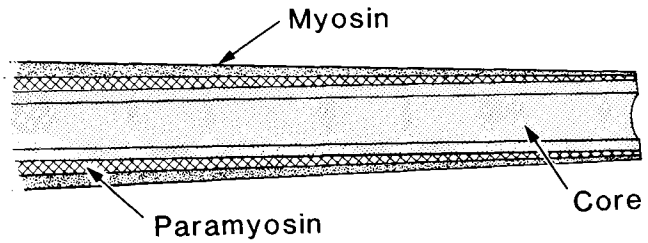

FIGURE 14 Schematic diagram of tapering domains. A sagittal section through the polar region of a thick filament is shown. The myosin and paramyosin domains are tapering whereas the tubular core structure remains constant. Note that the myosin and paramyosin domains cannot remain filled for much of the polar regions. Near the ends, all three structures must change radically. Not drawn to scale.

domains would be concentric annuli of 4 nm thickness about a core of 15 nm in diameter. Both myosin and paramyosin domains would then become progressively smaller towards the ends of the filaments. The thicknesses of myosin and paramyosin can only be considered estimates, and both domains may contain unidentified molecular components as well. We do not know whether paramyosin or the polar core structures extend through the central zones, or how far the paramyosin extends in the polar regions. Regardless of the exact dimensions and protein contents, the qualitative conclusions are that both the myosin and paramyosin domains must taper as the overall thick filament tapers (over several micrometers of length) and ultimately become discontinuous or disappear in the polar regions. The local structural relationships of myosin and paramyosin molecules in these domains must change significantly from the central to the polar regions.

Although the core structure appears constant in diameter, the internal density of the core appears to change along the filament length. The density of thick filaments appears consistently solid in the central regions, intermediate in the more polar regions, and hollow near the ends. An intriguing possibility is that the internal molecular components of the core structures are templates that determine the ultimate lengths of the polar core structures and, in turn, of the tapering paramyosin and myosin domains. Although this suggestion is a novel mechanism for length determination of thick filaments, the relevant morphological features of nematode body wall thick filaments, such as tapering and changes in core density, have been observed in a variety of thick filaments from other invertebrate muscles. These other thick filaments include those in specific muscles from other nematodes (8), lobsters (7), scallops (18), and various insects (5, 20). The results with the other invertebrate muscle thick filaments and the previous observations in *C. elegans* (26, 27) were interpreted in terms of pure myosin filaments or myosin-paramyosin co-filaments. The dissociation experiments that suggest our model were not performed in the previous studies. It is highly plausible that the core structures, their putative internal components, and the tapering of the myosin and paramyosin domains may be general features of invertebrate thick filaments. A core structure separate from myosin in all thick filaments has been proposed by Squire (23) based upon theoretical considerations of myosin packing and content.

Macromolecular templates have been proposed as length-determining mechanisms in virus assembly. The role of genomic RNA molecules in determining the stable length of tobacco mosaic virus particles appears reasonably clear (10). In the more complex viruses such as bacteriophages λ and T4, the H and GP48 proteins, respectively, have been proposed as possible templates for the determination of tail tube length (1, 9).

The observations regarding the domains of wild-type nematode thick filaments reported here pertain to studies of specific muscle-defective mutants of *C. elegans* and their structures related to thick filaments. Core structures are present in isolated thick filament-related structures (manuscript in preparation) from the E190 mutant that produces no myosin B (15, 22) and the E1214 mutant that produces no paramyosin (11, 27). These results support our conclusions that the core structure does not contain myosin B or paramyosin. In cross-sections of E1214 body wall muscles, many hollow tubular structures are observed (11, 27). These struc-

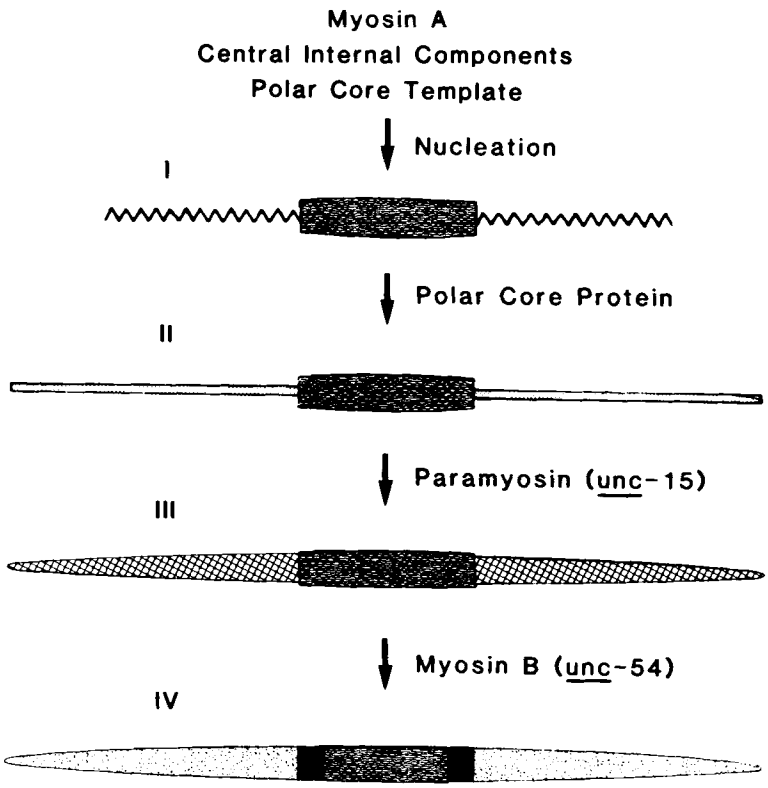

FIGURE 15 Pathway of thick filament assembly. Myosin A, polar core template, and central core components are required for nucleation (I). Polar core protein polymerizes about the polar core template to form the core structure (II). Paramyosin polymerizes about the polar core structure (III). Myosin B polymerizes about the paramyosin, and assembly terminates (IV). The polar core template, central internal components, and polar core protein are postulated and have not been identified biochemically.

tures are very similar in diameter and morphological appearance to the core structures and thick filament ends that we describe. The myosin-containing 1.5-μm-long bipolar filaments isolated from E1214 (11) resemble the myosin A central regions that we describe. The E73 mutant has paracrystalline structures in its body wall muscles (27) that resemble paracrystals of purified paramyosin prepared in vitro and the paracrystalline domains of thick filaments dissociated at 0.25 M KCl reported here.

The substructures of native- and dissociated-nematode body wall thick filaments described in this paper and similar structures observed in specific mutants suggest a possible set of intermediates in the pathway of assembly for the native filaments (Fig. 15). The myosin A-containing central regions appear to be the most stable structures. Together with whatever molecules form the internal core material and possibly paramyosin, myosin A would participate in the nucleation of thick filament assembly. The sequential polymerizations of core protein to form the polar core tube, of paramyosin to form the intermediate domains, and finally, of myosin B would likely follow such a nucleation during thick filament assembly. Myosins A and B would be contributing to the initial and terminal phases of assembly in wild-type nematodes, respectively. This model for the assembly of thick filaments will be tested in *C. elegans* by the analysis of structures related to thick filaments in specific muscle-defective mutants and by the isolation and characterization of postulated but presently unidentified molecular components.

We thank Drs. Sandra Honda, Roger Kornberg, Mathoor R. Sivaramakrishnan, and Laurel Traeger for discussions.

The research was supported by grants from the Jerry Lewis Neuromuscular Disease Research Center of the Muscular Dystrophy Association, the National Institute of Aging, and the National Institute of General Medical Sciences.

REFERENCES

1. Duda, R. L., and F. A., Eiserling. 1982. Evidence for an internal component of the bacteriophage T4D tail core. A possible length-determining template. *J. Virol.* 43:714–720.
2. Epstein, H. F., R. H. Waterston, and S. Brenner. 1974. A mutant affecting the heavy chain myosin in *Caenorhabditis elegans*. *J. Mol. Biol.* 90:291–300.
3. Epstein, H. F., D. M. Miller III, L. A. Gossett, and R. M. Hecht. 1982. Immunological studies of myosin isoforms in nematode embryos. *In* Muscle Development: Molecular and Cellular Control. M. L. Pearson and H. F. Epstein, editors. Cold Spring Harbor Laboratory, Cold Spring Harbor, New York. 7–14.
4. Garcea, R. L., F. Schachat, and H. F. Epstein. 1978. Coordinate synthesis of two myosins in wild-type and mutant nematode muscle during larval development. *Cell.* 15:421–428.
5. Goode, M. D. 1972. Ultrastructural and contractile properties of isolated myofibrils and myofilaments from *Drosophila* flight muscle. *Trans. Am. Microsc. Soc.* 91:182–194.
6. Harris, H. E., and H. F. Epstein. 1977. Myosin and paramyosin of *Caenorhabditis elegans*: biochemical and structural properties of wild-type and mutant proteins. *Cell.* 10:709–719.
7. Hayes, D., M. Huang, and C. R. Zobel. 1971. Electron microscope observations on thick filaments from the lobster *Homarus americanus*. *J. Ultrastruct. Res.* 37:17–30.
8. Hirumi, H., D. J. Raski, and N. O. Jones. 1971. Primitive muscle cells of nematodes: morphological aspects of platymyarian and shallow coelomyarian muscles in two plant parasitic nematodes, *Trichodorus christiei* and *Longidorus elongatus*. *J. Ultrastruct. Res.* 34:517–543.
9. Katsura, I. 1983. Tail assembly and injection. *In* Lambda II. R. W. Hendrix, J. W. Roberts, F. W. Stahl, and R. A. Weisberg, editors. Cold Spring Harbor Laboratory, Cold Spring Harbor, New York 331–346.
10. Klug, A. 1972. The polymorphisms of tobacco mosaic virus protein and its significance for the assembly of the virus. *Ciba Found. Symp.* 7:206–215.
11. Mackenzie, J. M., Jr., and H. F. Epstein. 1980. Paramyosin is necessary for determination of nematode thick filament length *in vivo*. *Cell.* 22:747–755.
12. Mackenzie, J. M., Jr., and H. F. Epstein. 1981. Electron microscopy of nematode thick filaments. *J. Ultrastruct. Res.* 76:277–285.
13. Mackenzie, J. M., Jr., F. Schachat, and H. F. Epstein. 1978. Immunocytochemical localization of two myosins within the same muscle cells in *Caenorhabditis elegans*. *Cell.* 15:413–419.
14. Mackenzie, J. M., Jr., R. L. Garcea, J. M. Zengel, and H. F. Epstein. 1978. Muscle development in *Caenorhabditis elegans*: mutants exhibiting retarded sarcomere construction. *Cell.* 15:751–762.
15. MacLeod, A. R., R. H. Waterston, R. M. Fishpool, and S. Brenner. 1977. Identification of the structural gene for a myosin heavy chain in *Caenorhabditis elegans*. *J. Mol. Biol.* 114:133–140.
16. McLachlan, A. D., and J. Karn. 1983. Periodic features in the amino acid sequence of nematode myosin rod. *J. Mol. Biol.* 164:605–626.
17. Miller, D. M. III, I. Ortiz, and G. C. Berliner, and H. F. Epstein. 1983. Differential localization of two myosins within nematode thick filaments. *Cell.* 34:477–490.
18. Millman, B. M., and P. M. Bennett. 1976. Structure of the cross-striated adductor muscle of the scallop. *J. Mol. Biol.* 103:439–467.
19. Niederman, R., and L. K. Peters. 1982. Native bare zone assemblage nucleates myosin filament assembly. *J. Mol. Biol.* 161:505–517.
20. Reedy, M. K., K. R. Leonard, R. Freeman, and T. Arad. 1981. Thick myofilament mass determination by electron scattering measurements with the scanning transmission

electron microscope. *J. Muscle Res. Cell Motil.* 2:45–64.
21. Schachat, F., R. L. Garcea, and H. F. Epstein. 1978. Myosins exist as homodimers of heavy chains: demonstration with specific antibody purified by nematode mutant myosin affinity chromatography. *Cell.* 15:405–411.
22. Schachat, F. H., H. E. Harris, and H. F. Epstein. 1977. Two homogeneous myosins in body-wall muscle of *Caenorhabditis elegans. Cell.* 10:721–728.
23. Squire, J. M. 1971. General model for the structure of all myosin-containing filaments. *Nature (Lond.).* 233:457–462.
24. Szent-Györgyi, A. G., C. Cohen, and J. Kendrick-Jones. 1971. Paramyosin and the filaments of molluscan "catch" muscles. II. Native filaments: isolation and characterization. *J. Mol. Biol.* 56:239–258.
25. Trinick, J., and J. Cooper. 1980. Sequential disassembly of vertebrate muscle thick filaments. *J. Mol. Biol.* 141:315–321.
26. Waterston, R. H., H. F. Epstein, and S. Brenner. 1974. Paramyosin of *Caenorhabditis elegans. J. Mol. Biol.* 90:285–290.
27. Waterston, R. H., R. M. Fishpool, and S. Brenner. 1977. Mutants affecting paramyosin in *Caenorhabditis elegans. J. Mol. Biol.* 117:828–842.
28. Waterston, R. H., D. G. Moerman, D. Baillie, and T. R. Lane. 1982. Mutations affecting myosin heavy chain accumulation and function in the nematode *Caenorhabditis elegans. In* Diseases of the Motor Unit. D. L. Schotland, editor. John Wiley and Sons, Inc., New York. 747–760.
29. Wray, J. S. 1979. Structure of the backbone in myosin filaments of muscle. *Nature (Lond.).* 277:37–40.
30. Zengel, J. M., and H. F. Epstein. 1980. Muscle development in *Caenorhabditis elegans*: a molecular genetic approach. *In* Nematodes as Model Biological Systems. B. M. Zuckerman, editor. Academic Press, Inc., New York. 76–126.